Far-infrared spectroscopy investigation of commensurate and incommensurate Cs_2CdBr_4 crystal

1999 J. Phys.: Condens. Matter 11 3601

(http://iopscience.iop.org/0953-8984/11/17/318)

J. Phys.: Condens. Matter **11** (1999) 3601–3613. Printed in the UK PII: S0953-8984(99)01520-9

Far-infrared spectroscopy investigation of commensurate and incommensurate Cs_2CdBr_4 crystal

Ya Shchur†‡, S Kamba‡ and J Petzelt‡

† Institute of Physical Optics, Dragomanova 23, Lviv, UA-290005, Ukraine
‡ Institute of Physics, Academy of Sciences of the Czech Republic, Na Slovance 2, 18221 Prague 8, Czech Republic

Received 2 February 1999

Abstract. Far-infrared reflectivity measurements of Cs_2CdBr_4 crystal were performed over the frequency region 15–600 cm^{-1} and temperature region 10–297 K. All transverse lattice modes have frequencies below 230 cm^{-1} because of the heavy atoms in the Cs_2CdBr_4 crystal. A sequence of phase transitions can be identified on the basis of the activation of new modes below the phase transition temperatures due to the lowering of the crystal symmetry on cooling. Factor-group analysis was carried out and selection rules found for the infrared activity of phonon modes in the incommensurate and commensurate phases, and the results were compared with the experimental data.

1. Introduction

Cs_2CdBr_4 crystal belongs to the rich group of well known A_2BX_4-type crystals. Due to the sequence of various phase transitions that they exhibit, the A_2BX_4 crystals have become viewed as almost model crystals for the investigation of structural phase transitions. A particular peculiarity of these crystals is the existence of an incommensurate (IC) phase between 237 and 208 K.

At room temperature, Cs_2CdBr_4 is isomorphous to β-K_2SO_4 crystal (space group $Pnma$, $Z = 4$ [1]). Upon cooling it undergoes several successive phase transitions. Summarizing the published data concerning x-ray investigations of Cs_2CdBr_4 structure [1, 3–6] and ^{81}Br NQR studies [2, 3, 7], one can identify the sequence of phase transitions shown as table 1.

Table 1. The sequence of phase transitions.

I	II (IC)	III	IV	V	VI
P_{nma}	$P_{1SS}^{P_{nma}}$	$P2_1/n11$	$P2_1/n11$	$P\bar{1}$	$P\bar{1}$
$Z = 4$	$k_i \approx 0.15$	$Z = 4$	or $P\bar{1}$, $Z = 4$	$Z = 4$	$Z = 8$
$T_1 = 252$ K	$T_2 = 237$ K	$T_3 = 208$ K	$T_4 = 156$ K	$T_5 = 130$ K	

The temperatures T_1, T_2 and T_4 of the phase transitions were observed by means of NQR studies [2, 3, 7]. Another phase transition at T_3 was found from dielectric measurements [4]. The observation of a new phase transition temperature at T_5 was reported later on the basis of an x-ray study [6].

0953-8984/99/173601+13$19.50

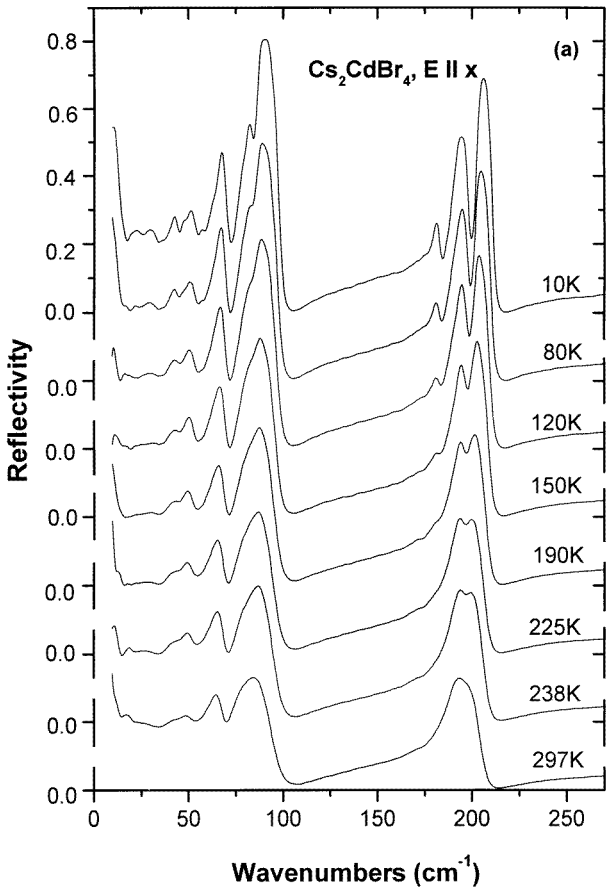

Figure 1. FIR reflectivity spectra of Cs_2CdBr_4 at different temperatures for (a) $\boldsymbol{E} \parallel \boldsymbol{x}$, (b) $\boldsymbol{E} \parallel \boldsymbol{y}$ and (c) $\boldsymbol{E} \parallel \boldsymbol{z}$ polarizations. The increase at the low-frequency end in some cases is an artefact caused by the partial transparency of the sample.

Condensation of a Σ_2 soft mode at the point $\boldsymbol{k}_i \approx 0.15\boldsymbol{a}^*$ of the Brillouin zone leads to an IC (II) phase with the $P^{P_{nma}}_{\bar{1}SS}$ symmetry (superspace-group notation) [3]. Using ^{81}Br NQR [2] and x-ray [5] investigations, it was shown that the soft-mode condensation causes a rotation by 7–8° around the $\boldsymbol{a}$-axis and a slight displacement in the $\boldsymbol{b}$-direction of all $CdBr_4^{2-}$ tetrahedra. From the optical observation of the effect of external stress on the domain structure, it was concluded that both the phases III and IV are ferroelastic [4]. The space group $P2_1/n11$ was proposed in references [2, 3, 5] for phases III and IV, but $P\bar{1}$ symmetry was established for phase IV in reference [4]. The space group $P\bar{1}$ was also proposed for the phase below 156 K [5] on the basis of x-ray measurements. But in a more recent x-ray study [6] the $P\bar{1}$ symmetry was confirmed only for phase VI below 130 K, while the symmetry of phase V was not established.

Although the acoustic properties and optical birefringence were studied in detail as functions of temperature and hydrostatic pressure [8, 9], and recently the temperature dependences of Raman [10, 11] and Brillouin [9] spectra were reported, infrared (IR) data and other lattice dynamics studies are lacking for Cs_2CdBr_4.

We set out to perform a complex study of the lattice dynamics of Cs_2CdBr_4 crystal

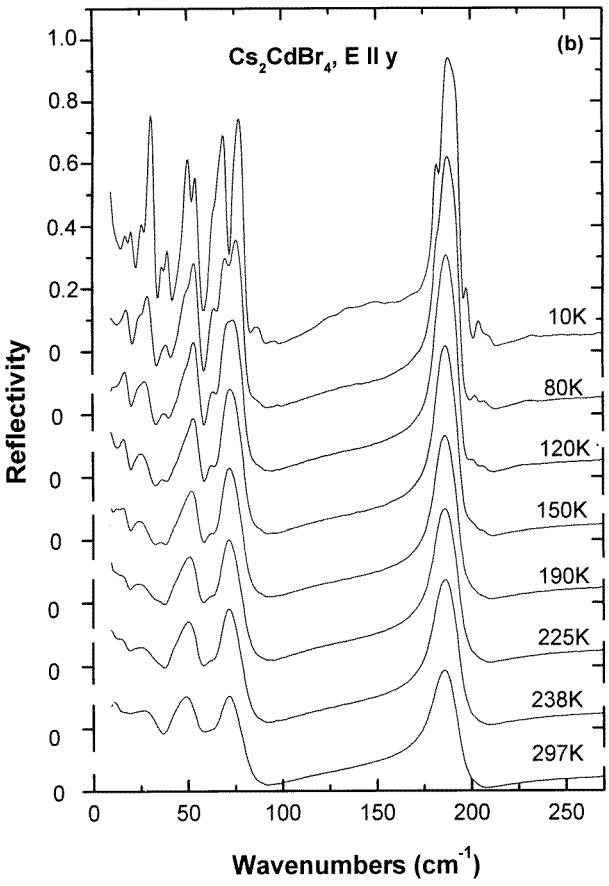

Figure 1. (Continued)

comprising experimental far-infrared (FIR) investigations over a wide temperature range and numerical simulation of lattice dynamics. In this paper we present the experimental results, their evaluation and a comparison with factor-group analysis. The data obtained will be used for lattice dynamics modelling in the following paper (paper II).

2. Experimental procedure

Cs_2CdBr_4 crystal was grown from the melt by the Czochralski method. The crystallographic axes were determined by x-ray diffraction. An easy cleavage was observed along the plane perpendicular to the $\boldsymbol{c}$-axis. Plane-parallel samples of (010) and (001) orientation of typical size $9 \times 7 \times 1$ mm^3 were cut and polished. Owing to sample cracking on polishing, we were unable to prepare samples thinner than 1 mm. Therefore we were unable to investigate the transmission spectra.

Near-normal polarized FIR reflectivity measurements (17–600 cm^{-1}) were performed using a Fourier transform interferometer, Bruker IFS 113v, at temperatures of 10–297 K. A liquid-helium-cooled Si bolometer operating at 1.5 K was used as a detector.

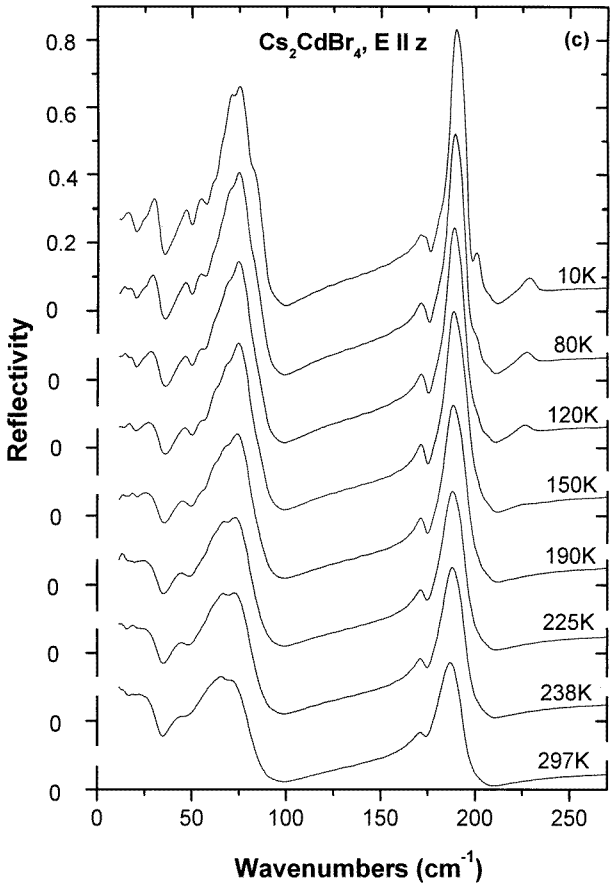

Figure 1. (Continued)

3. Results and evaluation

The FIR reflectivity spectra taken at various temperatures in the region 10–297 K for all three polarizations, $\boldsymbol{E} \parallel \boldsymbol{x}, \boldsymbol{y}, \boldsymbol{z}$, are shown in figure 1. The reflectivity spectra $R(\omega)$ were fitted with the well known formula [12]

$$R(\omega) \equiv \left| \frac{\sqrt{\varepsilon^*(\omega)} - 1}{\sqrt{\varepsilon^*(\omega)} + 1} \right|^2 \tag{1}$$

where the generalized four-parameter damped oscillator model [12] was used for the complex dielectric function:

$$\varepsilon^*(\omega) = \varepsilon'(\omega) + \mathrm{i}\varepsilon''(\omega) = \varepsilon_\infty \prod_j \frac{\Omega_{j\mathrm{LO}}^2 - \omega^2 + \mathrm{i}\gamma_{j\mathrm{LO}}\omega}{\Omega_{j\mathrm{TO}}^2 - \omega^2 + \mathrm{i}\gamma_{j\mathrm{TO}}\omega}. \tag{2}$$

Here ε_∞ denotes the high-frequency optical permittivity, $\Omega_{j\mathrm{TO}}$, $\Omega_{j\mathrm{LO}}$ are eigenfrequencies and $\Omega_{j\mathrm{TO}}$, $\Omega_{j\mathrm{LO}}$ damping constants of the transverse (TO) and longitudinal (LO) jth mode, respectively. This model is adequate for the description of overlapping and interacting modes with asymmetric phonon absorption line shapes. This situation may occur in the case of Cs_2CdBr_4 crystal owing to the overlap of the regions of external lattice vibrations of Cs^+ and

Table 2. Frequencies of the observed IR modes at 297 K (phase I) and 10 K (phase VI), and their symmetries. The letters vw, w, m, s and vs in parentheses indicate very weak, weak, medium, strong and very strong IR strength, respectively. The symmetry species are related to the phases I and VI at 297 and 10 K, respectively (see table 5, later).

$\boldsymbol{E} \parallel \boldsymbol{x}$		$\boldsymbol{E} \parallel \boldsymbol{y}$		$\boldsymbol{E} \parallel \boldsymbol{z}$	
10 K	297 K	10 K	297 K	10 K	297 K
A_u	B_{3u}	A_u	B_{2u}	A_u	B_{1u}
25(w)	—	18(w)	—	20(m)	—
32(w)	32(w)	20(w)	—	22(vw)	—
35(vw)	—	26(m)	—	30(s)	32(s)
44(m)	43(w)	30(vs)	32(s)	49(m)	44(m)
47(vw)	—	37(w)	—	54(m)	—
51(m)	49(m)	39(m)	—	61(m)	58(m)
57(vw)	—	49(s)	49(s)	65(w)	64(s)
62(m)	—	53(s)	—	69(s)	—
67(s)	65(s)	63(m)	61(w)	72(vs)	71(s)
79(s)	75(w)	66(vw)	—	80(s)	—
82(s)	—	68(vs)	—	159(w)	—
86(vs)	85(vs)	74(vs)	71(s)	172(m)	173(w)
182(m)	—	85(m)	—	174(vw)	—
191(s)	191(s)	94(w)	—	180(m)	—
202(s)	198(w)	182(s)	—	187(vs)	184(vs)
		186(vs)	183(s)	196(vw)	—
		196(m)	—	200(w)	200(vw)
		203(m)	—	203(vw)	—
		207(vw)	—	227(m)	—

Table 3. Compatibility relations among the irreducible representations along the main directions of the Brillouin zone in the *Pnma* (D_{2h}^{16}) phase ($0 < \mu_1, \mu_2, \mu_3 < 1/2$).

Γ ($\boldsymbol{k} = \boldsymbol{0}$)	Σ ($\boldsymbol{k} = \mu\boldsymbol{a}^*$)	X ($\boldsymbol{k} = \frac{1}{2}\boldsymbol{a}^*$)	Γ ($\boldsymbol{k} = \boldsymbol{0}$)	Δ ($\boldsymbol{k} = \mu\boldsymbol{b}^*$)	Y ($\boldsymbol{k} = \frac{1}{2}\boldsymbol{b}^*$)	Γ ($\boldsymbol{k} = \boldsymbol{0}$)	Λ ($\boldsymbol{k} = \mu\boldsymbol{c}^*$)	Z ($\boldsymbol{k} = \frac{1}{2}\boldsymbol{c}^*$)
$13A_g$			$13A_g$			$13A_g$		
	$26\Sigma_1$			$21\Delta_1$			$26\Lambda_1$	
$13B_{3u}$			$8B_{2u}$			$13B_{1u}$		
		$52X_1$			$42Y_1$			$52Z_1$
$13B_{2g}$			$8B_{1g}$			$13B_{2g}$		
	$26\Sigma_3$			$21\Delta_4$			$26\Lambda_4$	
$13B_{1u}$			$13B_{3u}$			$13B_{3u}$		
$8B_{3g}$			$13B_{2g}$			$8B_{1g}$		
	$16\Sigma_2$			$21\Delta_2$			$16\Lambda_2$	
$8A_u$			$8A_u$			$8A_u$		
		$32X_2$			$42Y_2$			$32Z_2$
$8B_{1g}$			$8B_{3g}$			$8B_{3g}$		
	$16\Sigma_4$			$21\Delta_3$			$16\Lambda_3$	
$8B_{2u}$			$13B_{1u}$			$8B_{2u}$		

$(CdBr_4)^{2-}$ ions and internal vibrations of $(CdBr_4)^{2-}$ groups. Furthermore, the values of the LO mode frequencies can be obtained from this model immediately.

The temperature dependences of TO mode frequencies for different symmetries evaluated from the FIR reflectivity spectra are presented in figure 2. These frequencies roughly

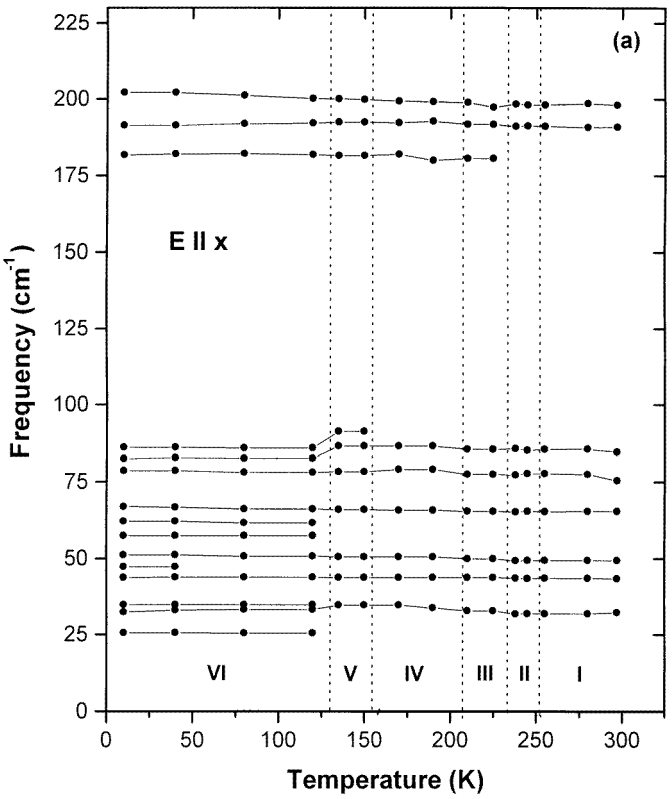

Figure 2. Temperature dependences of TO phonon frequencies calculated from the fits to (a) $\boldsymbol{E} \parallel \boldsymbol{x}$, (b) $\boldsymbol{E} \parallel \boldsymbol{y}$ and (c) $\boldsymbol{E} \parallel \boldsymbol{z}$ FIR reflectivity spectra.

correspond to frequencies of maxima in dielectric loss spectra, $\varepsilon''(\omega)$, which were calculated from the fit to the reflectivity spectra shown in figure 1 and are depicted in figure 3. The values of the TO frequencies obtained for marginal temperatures (room temperature and 10 K), and their classification is shown in table 2.

4. Discussion

According to the factor-group analysis, in the high-temperature phase I [11] the 84 vibrational modes of Cs_2CdBr_4 crystal at the Brillouin zone centre are classified in terms of irreducible representations as follows:

$$\Gamma(\mathrm{I}) = 13\mathrm{A_g} + 8\mathrm{B_{1g}} + 13\mathrm{B_{2g}} + 8\mathrm{B_{3g}} + 8\mathrm{A_u} + 13\mathrm{B_{1u}} + 8\mathrm{B_{2u}} + 13\mathrm{B_{3u}} \qquad (3)$$

including the $1\mathrm{B_{1u}} + 1\mathrm{B_{2u}} + 1\mathrm{B_{3u}}$ acoustic modes. The rest of the $\mathrm{B_{1u}}$, $\mathrm{B_{2u}}$ and $\mathrm{B_{3u}}$ modes are IR active, while all modes with gerade (g) symmetry are Raman active. The modes of $\mathrm{A_u}$ symmetry are silent in Raman and IR spectra in this phase. All of the mode activities are summarized in table 3.

For the mode classification (3), we have taken into account external and internal vibrations together, because all of the observed modes lie in the low-frequency region below 230 cm^{-1} due to the large mass of structural units of this crystal. According to references [11, 13–15], the $CdBr_4^{2-}$ groups have very low-frequency bending vibrations in the regions 49–53 cm^{-1} (ν_2) and

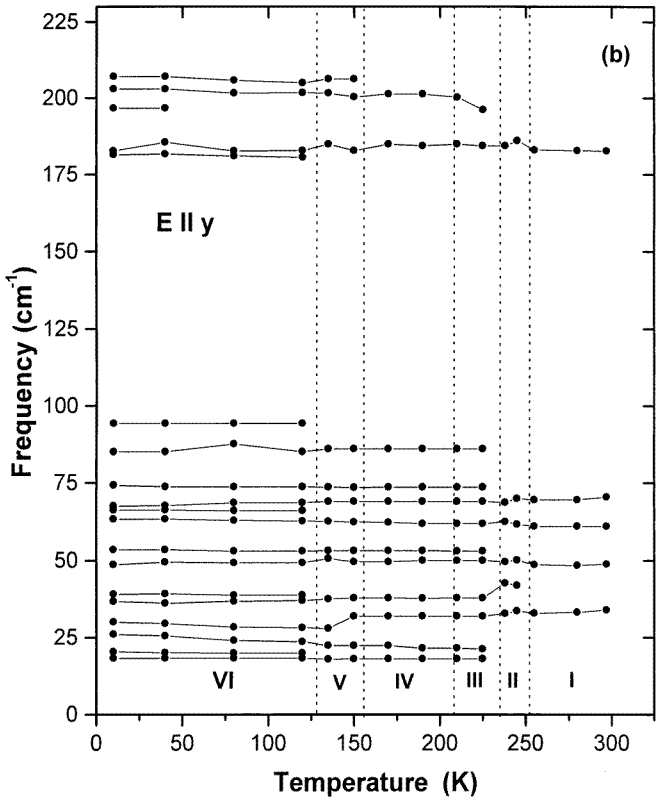

Figure 2. (Continued)

61–75 cm^{-1} (ν_4) and stretching vibrations in the regions 161–166 cm^{-1} (ν_1) and 177–181 cm^{-1} (ν_3). Analogously to the case for other representatives of the A_2BX_4 family (e.g. Cs_2HgCl_4), we can suppose that the external lattice vibrations of Cs_2CdBr_4 crystal lie below 90 cm^{-1}. This implies that in the region of 50–90 cm^{-1} the external and internal bending vibrations are mixed together and most probably overlapped. Due to this, the number of observed lines is much smaller than theoretically predicted. As one can see from figures 1 and 2, the IR spectra for all polarizations are localized in two separate parts. In the low-frequency part below 90 cm^{-1}, it seems to us, there are external and internal (bending) vibrations and in the high-frequency part (between 170 and 230 cm^{-1}) strong pure internal (stretching) vibrations of $CdBr_4^{2-}$ groups are observed.

As one can see from figures 1 and 2, no new modes are observed in FIR spectra for $\boldsymbol{E} \parallel \boldsymbol{x}$ and $\boldsymbol{E} \parallel \boldsymbol{z}$ polarizations in the IC phase below $T_i = 253$ K. Only one weak mode appears, at 43 cm^{-1}, in the $\boldsymbol{E} \parallel \boldsymbol{y}$ spectrum of the IC phase. This mode is activated from the Brillouin zone centre (the Γ point) because it remains active in the FIR spectra also in non-modulated phases at lower temperatures. The mode is probably IR active already in phase I, and it appears in the spectra of the IC phase only due to lower phonon damping at low temperatures.

It is known [16] that the condensation of a soft mode at some intermediate point of the Brillouin zone with an irrational value $\boldsymbol{k}_i$ of the wave vector, leading to a phase transition into the modulated phase, induces the appearance of IR- or Raman-active modes at $\pm m\boldsymbol{k}_i$ ($m = 1, 2, \ldots$; $\boldsymbol{k}_i$ is the wave vector of the frozen-in soft mode) which were inactive in the same spectra

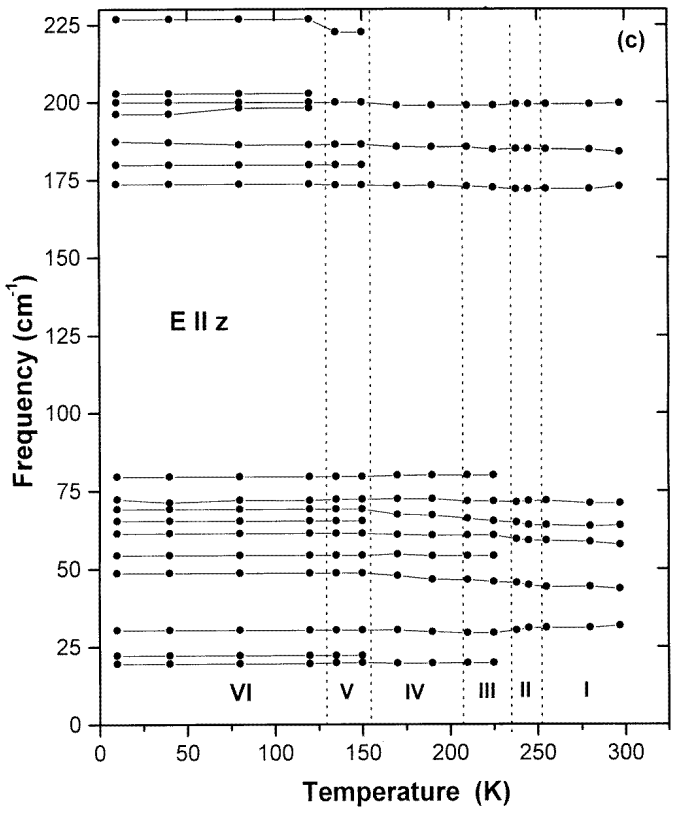

Figure 2. (Continued)

in phase I. The activation of the new modes in the IC phase takes place owing to the bilinear coupling between these modes and those from the Brillouin zone centre active in phase I.

To find the symmetry type and activity of the phonon modes at $\pm m\boldsymbol{k}_i$ in the IC phase, one has to determine the corresponding bilinear coupling terms in the thermodynamic potential of the IC phase. To do this, one has to decompose the direct product $[\Sigma_2]^m \otimes \Sigma_i$ into irreducible representations, where Σ_2 and Σ_i ($i = 1, \ldots, 4$) are irreducible representations of the soft mode and the mode of wave vector $\boldsymbol{k} = \mu\boldsymbol{a}^*$ ($0 < \mu < 1/2$) whose activity we investigate, respectively ($[\cdots]^m$ denotes the symmetrized mth power [16]). Only those products which have the resulting $\boldsymbol{k}$-vector equal to zero have to be considered. Then the corresponding irreducible representations are point-group representations at the Γ point and directly determine the activity of the mode in question. To perform the above-mentioned analysis, we have used the compatibility relations among irreducible representations along the Σ direction ($\boldsymbol{k} = \mu\boldsymbol{a}^*$) of the phase-I Brillouin zone. These are listed (together with compatibilities along the Δ ($\boldsymbol{k} = \mu\boldsymbol{b}^*$) and Λ ($\boldsymbol{k} = \mu\boldsymbol{c}^*$) lines) in table 3.

The results of our analysis at wave vectors $\boldsymbol{k}_i$, $2\boldsymbol{k}_i$ and $3\boldsymbol{k}_i$ are presented in table 4. It should be noted that the strength of activated modes at $\boldsymbol{k}_i$ is proportional to η^2 while the strengths of those at $2\boldsymbol{k}_i$ and $3\boldsymbol{k}_i$ are proportional to η^4 and η^6, respectively, where η is the order parameter (the amplitude of the frozen-in soft mode).

From table 4 one can see that, to a first approximation (modes from $\pm\boldsymbol{k}_i$ whose IR strength is proportional to η^2), 16, 26 and 16 new IR modes are active in the $\boldsymbol{E} \parallel \boldsymbol{x}, \boldsymbol{y}, \boldsymbol{z}$ spectra,

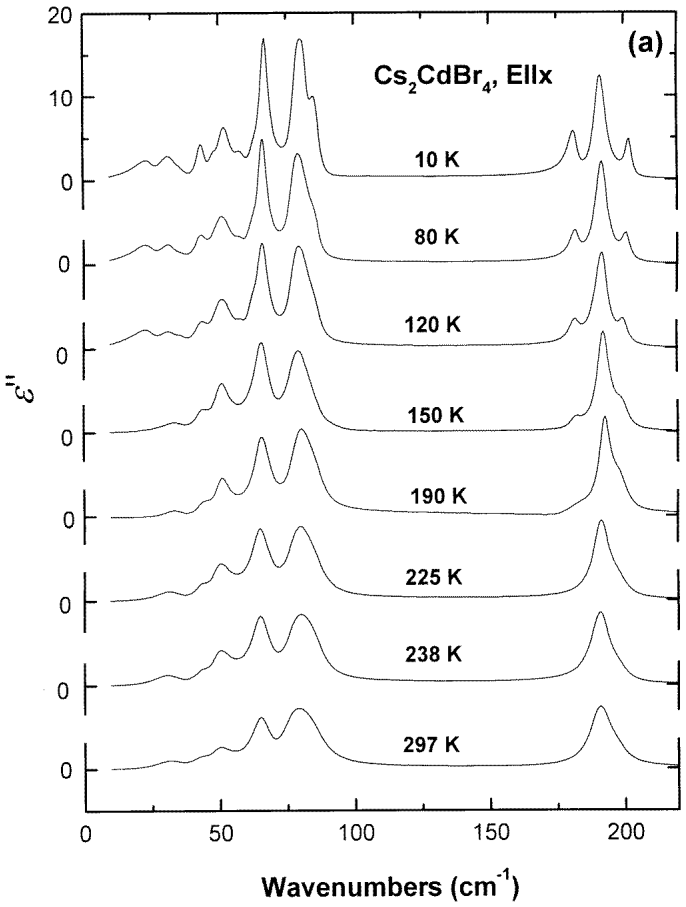

Figure 3. Dielectric loss ($\varepsilon''(\omega)$) spectra calculated from the fits to the reflectivity spectra shown in figure 1.

Table 4. Symmetries and numbers of phonon branches in different spectra in the IC phase activated by the frozen Σ_2 soft mode.

Activity	$\boldsymbol{k}_i$	$2\boldsymbol{k}_i$	$3\boldsymbol{k}_i$
$A_g(xx, yy, zz)$	$16\Sigma_2$	$26\Sigma_1$	$16\Sigma_2$
$B_{3u}(x)$	$16\Sigma_2$	$26\Sigma_1$	$16\Sigma_2$
$B_{3g}(yz)$	$26\Sigma_1$	$16\Sigma_2$	$26\Sigma_1$
A_u(—)	$26\Sigma_1$	$16\Sigma_2$	$26\Sigma_1$
$B_{2g}(xz)$	$16\Sigma_4$	$26\Sigma_3$	$16\Sigma_4$
$B_{1u}(z)$	$16\Sigma_4$	$26\Sigma_3$	$16\Sigma_4$
$B_{1g}(xy)$	$26\Sigma_3$	$16\Sigma_4$	$26\Sigma_3$
$B_{2u}(y)$	$26\Sigma_3$	$16\Sigma_4$	$26\Sigma_3$

respectively. The degeneracy of modes at $\boldsymbol{k}_i$ and $-\boldsymbol{k}_i$ existing in phase I is lifted in the IC phase due to the interaction with the frozen soft mode.

The specific lattice excitations in the IC phase, the long-wavelength amplitudon and phason, are not IR active, but are only Raman active [16]. The amplitudon should be active in

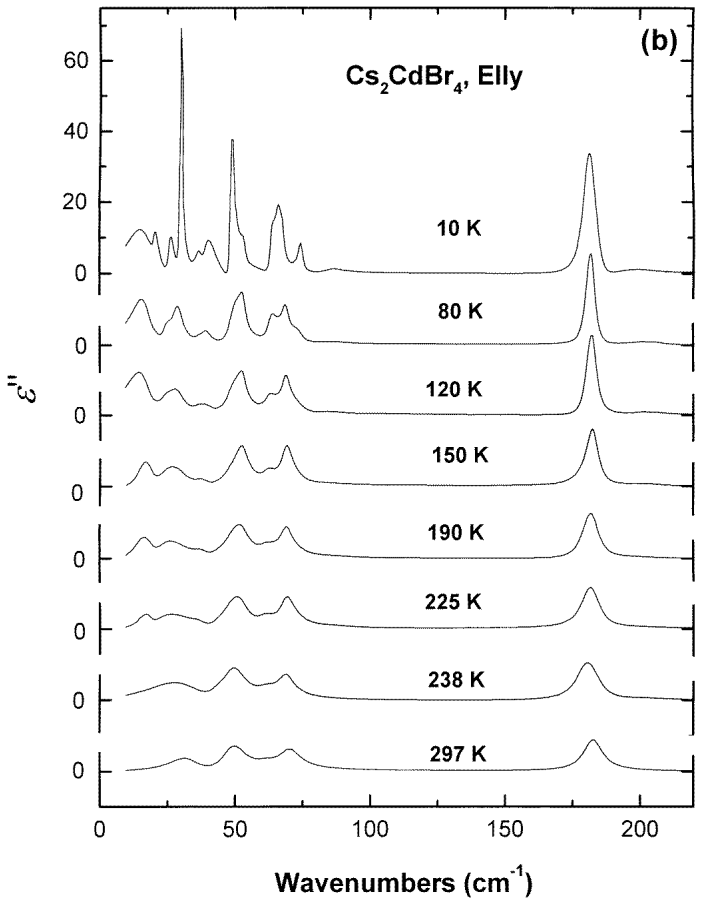

Figure 3. (Continued)

the totally symmetric A_g spectra and the phason in the A_g, B_{1g} and B_{2g} spectra for propagation along the x-, y- and z-axes, respectively [17, 18]. However, no significant changes in the Raman spectra were seen at the I–II transition, and neither of these modes were detected, from which it was concluded that the transition is of the order–disorder type [10, 11].

The phase transition from the IC to the monoclinic phase III (space group $P2_1/n$) is accompanied by the appearance of new lines in the IR spectra. As one can see from figures 1 and 2, one new stretching mode in the $\boldsymbol{E} \parallel \boldsymbol{x}$ spectrum, six new ones in the $\boldsymbol{E} \parallel \boldsymbol{y}$ spectrum and three new ones in the $\boldsymbol{E} \parallel \boldsymbol{z}$ spectrum are observed at $T = 225$ K. The appearance of new modes in this phase can be explained using the correlation diagram for the irreducible representations of phases I, III and V (table 5). As one can see from table 5 [11], the total number of normal modes of both A_u and B_u symmetry must increase to 21 at the direct I–III phase transition. It should be noted that the modes of A_u which are symmetry forbidden in IR and Raman spectra in phase I, according to the selection rules, become allowed in the $\boldsymbol{E} \parallel \boldsymbol{x}$ IR spectra in phase III. But no dramatic changes in this spectrum are seen.

It is also the case that no significant changes in spectra of any polarizations are observed at the III–IV phase transition. This speaks in favour of the $P2_1/n$ symmetry for phase IV, for which either the $P2_1/n$ or the $P\bar{1}$ space group was proposed on the basis of x-ray measurements [6].

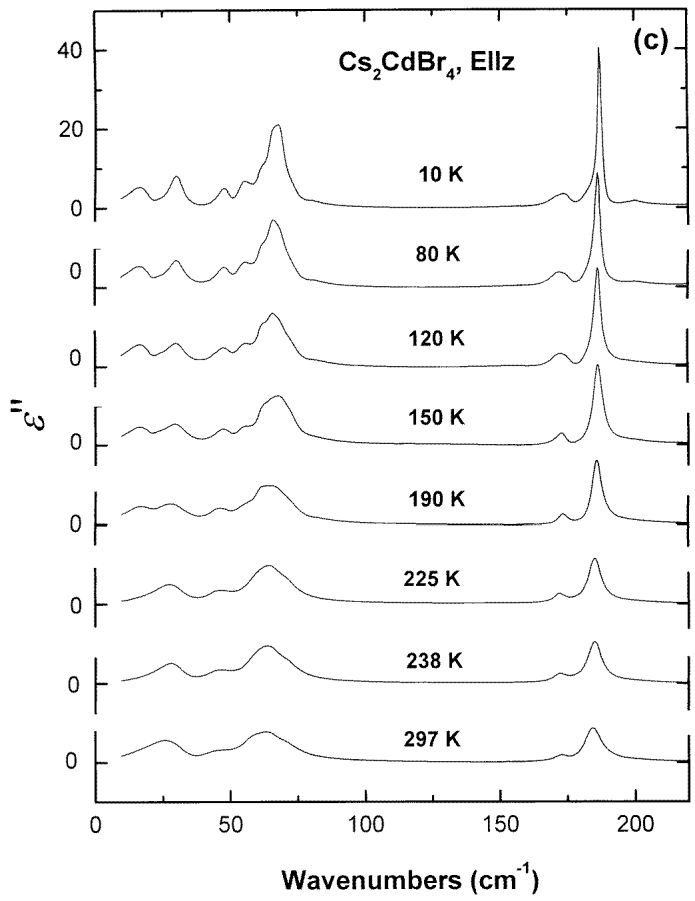

Figure 3. (Continued)

The IV–V phase transition to the triclinic $P\bar{1}$ phase is accompanied by the observation of six new IR modes. The number of symmetry-allowed modes in phase V increases to 42 (table 5). The observation of new frequencies of $CdBr_4^{2-}$ stretching vibrations at $T = 150$ K in phase V (180 and 224 cm^{-1} for $\boldsymbol{E} \parallel \boldsymbol{z}$ polarization and at 208 cm^{-1} for $\boldsymbol{E} \parallel \boldsymbol{y}$ polarization) indicates the change of the site symmetry of the $CdBr_4^{2-}$ group and some deformation of these groups. It is worth noting that an underdamped soft mode was observed in the Raman spectra (A_g symmetry in phase IV) at this phase transition, which allowed us to reach the conclusion that the IV–V phase transition has displacive character [10, 11].

The appearance of new modes and a significant narrowing of the lines is observed in IR spectra for all polarizations at the lowest-temperature V–VI phase transition. In reference [11], an assumption was made that the unit-cell volume was doubled due to the soft-mode condensation at the $(1/2)(\boldsymbol{b}^* + \boldsymbol{c}^*)$ point of the Brillouin zone boundary, in analogy with the cases of Cs_2HgBr_4, Rb_2ZnCl_4 and K_2ZnCl_4 crystals [19]. If this assumption is correct (see the factor-group analysis in table 5), it could explain the observed considerable enrichment of the IR spectra (four, six and two new modes for $\boldsymbol{E} \parallel \boldsymbol{x}, \boldsymbol{y}, \boldsymbol{z}$ polarization, respectively—see figure 2) at low temperatures.

Table 5. The correlation diagram for irreducible representations in the commensurate phases I, III, IV, V and VI (after reference [11]).

I	III, IV	V	VI
P_{nma} (D_{2h}^{16})	$P2_1/n11$ (C_{2h}^{5})	$P\bar{1}$ (C_i^1)	$P\bar{1}$ (C_i^1)
$13A_g(xx, yy, zz)$			
	$21A_g(xx, yy, zz, yz)$		
$8B_{3g}(yz)$			
		$42A_g(xx, yy, zz, yz, xy, xz)$	$84A_g(xx, yy, zz, yz, xy, xz)$
$8B_{1g}(xy)$			
	$21B_g(xy, xz)$		
$13B_{2g}(xz)$			
$8A_u$(—)			
	$21A_u(x)$		
$13B_{3u}(x)$			
		$42A_u(x, y, z)$	$84A_u(x, y, z)$
$13B_{1u}(z)$			
	$21B_u(y, z)$		
$8B_{2u}(y)$			

5. Conclusions

Far-infrared reflectivity data enabled us to determine the dielectric function and polar mode frequencies of Cs_2CdBr_4 crystals in all of the six known phases between room temperature and 10 K. Activation of a new weak mode was observed for $\boldsymbol{E} \parallel \boldsymbol{y}$ polarization at the phase transition to the IC phase. However, this mode also remained active in the spectra at lower temperatures (in non-modulated phases); therefore it belongs to the Brillouin zone centre. No new modes with wave vector $\boldsymbol{q} = \pm m\boldsymbol{k}_i$ are seen in the IC phase, obviously due to their low oscillator strengths. Nevertheless, the symmetry and number of new phonon modes which can be theoretically activated by the freezing of the Σ_2 soft-phonon branch were determined using group theory. Due to the absence of any changes in the IR spectra at the III–IV phase transition, the monoclinic $P2_1/n11$ symmetry of phase IV ($208 > T > 156$ K) is more probable than the triclinic $P\bar{1}$ one. The appearance of new internal vibrations in phase V probably implies deformation of the $CdBr_4^{2-}$ groups due to the lowering of the site symmetry at least to $P\bar{1}$. The existence of the questionable last phase transition at T_5 was clearly confirmed by the activation of eleven new modes in our FIR spectra.

Acknowledgments

The authors wish to thank Dr Ya Burak from the Institute of Physical Optics in Lviv for providing them with good-quality Cs_2CdBr_4 crystal for the IR measurements and V Dvorak for helpful discussions. The work was supported by the Grant Agency of the Czech Republic (project No 202/98/1282), the Grant Agency of the Academy of Science (project No A1010828) and the Czech Ministry of Education (project Kontakt ME 100) which enabled one of us (YaS) to realize a stay at the Institute of Physics, Prague.

References

[1] Altermatt D, Arend H, Niggli A and Pretter W 1979 *Mater. Res. Bull.* **14** 1391
[2] Plesko S, Kind R and Arend H 1980 *Ferroelectrics* **26** 703

[3] Plesko S, Kind R and Arend H 1980 *Phys. Status Solidi* a **61** 87
Plesko S 1981 *Thesis* Swiss Federal Institute of Technology, Zurich
[4] Maeda M, Honda A and Yamada N 1983 *J. Phys. Soc. Japan* **52** 3219
[5] Altermatt D, Arend H, Gramlich V, Niggli A and Petter W 1984 *Acta Crystallogr.* B **40** 347
[6] Zaretskii V and Depmeier W 1991 *7th European Mtg on Ferroelectricity* (Dijon: University of Burgundy Press) abstract 207
[7] Nakayama N, Nakamura N and Chihara H 1986 *Z. Naturf.* a **41** 261
[8] Kityk A V, Mokry O M, Soprunyuk V P and Vlokh O G 1993 *J. Phys.: Condens. Matter* **5** 5189
[9] Kuzel P, Moch P, Gomez-Cuevas A and Dvorak V 1994 *Phys. Rev.* B **49** 6553
Kuzel P, Dvorak V and Moch P 1994 *Phys. Rev.* B **49** 6563
[10] Rodriguez V, Couzi M, Gomez-Cuevas A and Chaminade J P 1991 *Phase Transitions* **31** 75
[11] Torgashev I, Yuzyuk Yu I, Burmistrova L A, Smutny F and Vanek P 1993 *J. Phys.: Condens. Matter* **5** 5761
[12] Gervais F 1983 *Infrared and Millimeter Waves* vol 8, ed K J Button (New York: Academic) p 435
[13] Ross S D, Siddiqi I W and Tyrell H J 1972 *J. Chem. Soc. Dalton Trans.* 1613
[14] Goddin P L, Goodfellow R J and Kessler K 1977 *J. Chem. Soc. Dalton Trans.* 1914
[15] Nakamoto K 1978 *Infrared and Raman Spectra of Inorganic and Coordination Compounds* (New York: Wiley)
[16] Petzelt J 1981 *Phase Transitions* **2** 155
[17] Poulet H and Pick R M 1981 *J. Phys. C: Solid State Phys.* **14** 2675
[18] Poulet H and Pick R M 1986 *Fundamentals (Incommensurate Phases in Dielectrics vol 1)* ed R Blinc and A P Levanyuk (Amsterdam: Elsevier–Science) pp 315–35
[19] Quilichini M, Dvorak V and Boutroville P 1991 *J. Physique* **1** 1321